The Open Dentistry Journal
DOI: 10.2174/0118742106360054250425112022, 2025, 19, e18742106360054
ISSN: 1874-2106

RESEARCH ARTICLE OPEN ACCESS

Comparative Investigation of the Antimicrobial Effects of Cerium Complex with Black and Green Tea Extracts

Zahra Esmaeili Moghaddam[1], Samin Hamidi[2,*], Sara Salatin[3] and Parina Asgharian[4,*]

[1]*Student Research Committee, Tabriz University of Medical Sciences, Tabriz, Iran*
[2]*Research Center of Psychiatry and Behavioral Sciences, Tabriz University of Medical Sciences, Tabriz, Iran*
[3]*Neurosciences Research Center, Tabriz University of Medical Sciences, Tabriz, Iran*
[4]*Department of Pharmacognosy, Faculty of Pharmacy, Tabriz University of Medical Sciences, Tabriz, Iran*

Abstract:

Background: Dental floss functionality can be enhanced to provide additional benefits beyond mechanical plaque removal. Novel coating techniques offer the potential for delivering antimicrobial and anti-inflammatory agents directly to interdental spaces.

Objective: The objective of this study is to develop and evaluate a dual-layer coating of polydopamine [PDA] and cerium-tea complex on dental floss for improved functionality and antimicrobial properties.

Methods: Cerium complexes with black tea [Ce-BT] and green tea [Ce-GT] extracts were synthesized using a green synthesis method. The coatings were characterized using FTIR spectroscopy, SEM-EDX analysis, and DLS. Coated floss was evaluated for weight increase, tensile strength, and coating transfer. Antimicrobial assays were conducted against *Escherichia coli*, *Staphylococcus aureus*, *Candida albicans*, *Streptococcus mutans* and P*orphyromonas gingivalis*.

Results: TIR confirmed successful complex formation between Ce^{3+} ions and tea polyphenols. SEM imaging revealed amorphous structures on coated threads, while EDX analysis confirmed the presence of cerium. The dual-layer coating significantly increased floss weight [53.69% total increase] and improved its tensile strength. Simulated flossing tests demonstrated coating transfer to interdental spaces. Antimicrobial assays showed strong inhibition against tested microorganisms, with Ce-GT exhibiting superior antimicrobial properties compared to Ce-BT. In addition, Ce-BT and Ce-GT coated silk threads showed greater antimicrobial properties in inhibiting the growth of selected microbial strains when compared with a control group of 0.12% chlorhexidine coated silk threads, although there was no significant difference between the groups when tested with one-way ANOVA. The coated floss maintained appropriate mechanical properties for dental applications.

Conclusion: This innovative dual-layer coating approach presents a promising method for delivering antibacterial and anti-inflammatory agents directly to interdental spaces, potentially offering an effective over-the-counter solution for periodontal disease prevention and treatment. Future research should focus on optimizing the coating process, evaluating efficacy against specific oral pathogens, and conducting *in vivo* studies to assess clinical outcomes.

Keywords: Antimicrobial, Black tea, Cerium complex, Dental floss, Dentistry, Green tea, Orthodontics, Polydopamine.

*Address correspondence to these authors at the Research Center of Psychiatry and Behavioral Sciences, Tabriz University of Medical Sciences, Tabriz, Iran; Tel: +98 41 33372250 and Department of Pharmacognosy, Faculty of Pharmacy, Tabriz University of Medical Sciences, Tabriz, Iran; E-mails: hamidisamin@gmail.com and parina.asgharian@gmail.com

Cite as: Moghaddam Z, Hamidi S, Salatin S, Asgharian P. Comparative Investigation of the Antimicrobial Effects of Cerium Complex with Black and Green Tea Extracts. Open Dent J, 2025; 19: e18742106360054.
http://dx.doi.org/10.2174/0118742106360054250425112022

Received: October 01, 2024
Revised: December 23, 2024
Accepted: March 05, 2025
Published: May 12, 2025

1. INTRODUCTION

Periodontitis, a common and irreversible disease affecting oral health-related quality of life, affects approximately half of the adult population in the United States. It can lead to systemic inflammation, contributing to other conditions such as cardiovascular disease, diabetes, and rheumatoid arthritis [1, 2].

Daily removal of bacterial plaque biofilm in the subgingival region is essential for preventing and treating periodontitis [3, 4]. Regular toothbrushes can't reach all areas between teeth, so tools like interdental brushes and dental floss are needed for proper interdental cleaning [3]. Since patients can apply the dental floss themselves at home, it could enhance patient adherence, alleviate discomfort, and lower medical expenses.

While dental floss is widely used in daily oral care, research reviews have found limited evidence of its effectiveness in reducing plaque buildup and gum inflammation when used alongside brushing [5-7]. Recent studies are exploring the addition of bioactive therapeutic compounds to dental floss to enhance its antimicrobial properties [8, 9].

Kaewiad *et al*. found that dental floss with an antibacterial agent can stop bacterial growth on agar plates [10], and Muniz *et al*. proved that chlorhexidine-impregnated dental floss reduces supragingival plaque in clinical trials [11, 12].

Recent studies have explored novel dental floss coatings for antimicrobial action and early caries detection [9]. While some commercial flosses claim antimicrobial properties, safety concerns persist due to their polytetrafluoroethylene or wax composition [13, 14]. Additionally, certain coatings, such as triclosan, have shown limited efficacy [15] and raised health concerns [16].

This necessitates the development of safer, effective antibacterial dental floss alternatives. Previous research on gold nanoparticle-coated floss demonstrated antimicrobial properties but lacked data on coating durability and floss functionality [17]. Other studies have primarily focused on periodontal disease rather than dental caries [9, 18].

A recent patent proposes floss coatings using natural polymers and metal nanoparticles [Cu, Ag, Li] to target both periodontal disease and dental caries, claiming antibacterial, antifungal, and immunostimulatory effects [19]. However, further research is needed to validate these claims and ensure long-term safety and efficacy.

Cerium, a rare earth element, has garnered attention due to its cost-effectiveness and abundance [20]. Cerium and cerium oxide-based nanomaterials, characterized by low toxicity, function as potent antibacterial agents due to their unique mechanism of action against pathogens involving the reversible conversion between Ce[III] and Ce[IV] oxidation states [21].

The combination of cerium with tea extracts through green synthesis methods offers a potential avenue for developing novel antibacterial agents for use in medical and healthcare products, such as dental floss.

The green synthesis method is both dynamic and energy-efficient, making it suitable for large-scale industrial production of nanoparticles [22]. Phytochemicals in the bio-extract confer antibacterial, antifungal, anticancer, anti-inflammatory, antioxidant, and catalytic properties to the green-synthesized nanoparticles [23, 24]. These characteristics have led to an increasing preference for green synthesis methods over traditional approaches [22].

Polydopamine's unique adhesive properties stem from its catechol-rich structure, enabling strong interactions with diverse surfaces. This characteristic makes it ideal for anchoring metal-based nanoparticles to polymeric dental floss. Its self-polymerizing nature could create a robust interfacial layer between floss and nanoparticles, potentially enhancing coating integrity and durability. Polydopamine's ability to bond with both organic and inorganic materials may promote more stable, uniform nanoparticle distribution on the floss surface, possibly improving the antimicrobial coating's effectiveness and longevity.

Coating techniques developed for polymeric sutures and wound dressings can be adapted and utilized for enhancing dental floss [25, 26]. This cross-application of methodologies from related medical fields offers promising avenues for improving floss functionality.

The primary objective of our research is to develop an innovative dental floss by applying a dual-layer coating to unwaxed nylon floss. This coating consists of an initial layer of polydopamine followed by a layer of cerium tea complex. To the best of our knowledge, this specific approach to enhancing interproximal oral care has not been previously explored, potentially offering a novel solution to address the limitations of conventional dental flossing products.

Our study represents a unique contribution to the rapidly evolving field of advanced materials in preventive dentistry. By harnessing the properties of polydopamine as an adhesive base layer and combining it with the antibacterial potential of a cerium tea complex, we aim to create a more effective tool for interdental cleaning and protection.

This research not only builds upon the growing body of work investigating bioactive coatings in oral care but also introduces a new direction by incorporating cerium, a rare earth element, in combination with natural tea extracts. Our approach aligns with the increasing interest in green synthesis methods and the application of bioactive compounds in restorative and preventive dentistry.

By developing this novel dental floss, we seek to provide a more efficient means of delivering beneficial agents to the crucial yet hard-to-reach interproximal spaces. This could potentially offer improved protection against dental caries and periodontal diseases, addressing a significant gap in current oral hygiene practices. The green synthesis method employed offers a cost-effective, eco-friendly, and biocompatible process, aligning with the growing preference for sustainable approaches in nanomaterial production [27].

2. MATERIALS AND METHODS

2.1. General Materials

Black tea [Camellia sinensis var. assamica] and green tea [Camellia sinensis var. sinensis] leaves were sourced from a commercial supplier in Tabriz, Iran. Dopamine hydrochloride [$C_8H_{11}NO_2$·HCl, ≥98% purity] and cerium

[III] nitrate hexahydrate [$Ce[NO_3]_3 \cdot 6H2O$, 99.99% trace metals basis, CAS Number 10294-41-4, Molecular Weight = 434.23 g/mol] were purchased from Merck [Darmstadt, Germany]. All other chemicals used were of analytical grade and used without further purification. Deionized water was used throughout the experiments.

To compare the effectiveness of the experimental group against a control group, GraphPad Prism version 10.4.1 [627] was used to conduct one-way ANOVA tests.

2.2. Preparation of Black and Green Tea Extract

Aqueous extracts of black and green tea were prepared as follows. For each tea variety, 4.0 g [±0.1 g] of dried tea leaves were finely ground using a mechanical grinder. The powdered leaves were then mixed with 25.0 mL of deionized water at 90°C [±1°C] in amber glass beakers to minimize light exposure. The mixtures were stirred continuously at 300 rpm for 10 minutes using a magnetic stirrer. Subsequently, the solutions were allowed to cool to room temperature [23°C ±2°C] for 30 minutes. The cooled extracts were then filtered through Whatman No. 41 filter paper [pore size: 20-25 µm, GE Healthcare, cat. no. 1441-125] to remove particulate matter. The resulting filtrates were collected in clean, labeled containers and stored at 4°C until further use [28].

2.3. Preparation of the Coating Material

Dental floss samples [15 ± 0.1 cm] were extracted from a commercial roll and secured at both ends to prevent fiber fraying. Floss segments were kept on the ruler using clips. To enhance the adhesion of the synthesized complex to the silk thread surface, a polydopamine [PDA] coating was applied. A dopamine solution [2 mg/L] was prepared, into which 2 cm segments of silk thread were immersed and stirred at 23°C ± 2°C in darkness for 24 hours. The observed darkening of the thread surface to gray indicated successful dopamine self-polymerization [29]. The PDA-coated threads were then rinsed three times with deionized water and dried in a vacuum oven at 25°C ± 1°C. Concurrently, a cerium nitrate solution was prepared by dissolving $Ce[NO_3]_3$ [1.0 g ± 0.1 g] in 10.0 mL of deionized water. The Ce[III]-complex synthesis and coating process were performed simultaneously by immersing 2 cm of PDA-coated silk thread in the cerium nitrate solution, to which the previously prepared tea extract was slowly added at 60°C ± 1°C under continuous stirring for 24 hours. The reaction progress was visually monitored, with the tea solution changing from dark to green, accompanied by the formation of a cloudy precipitate at the bottom of the reaction vessel, indicative of the formation of Ce-BT [Cerium-Black Tea] and Ce-GT [Cerium-Green Tea] complexes [18, 28].

Sample masses were determined using an analytical balance [Gemini GR-200, A&D, Japan; precision: ±0.1 mg] before and after coating application. The coating mass was calculated as the difference between these measurements, and the percentage weight change was computed [n = 6 per group].

Coated and uncoated floss samples underwent comprehensive characterization using:

Scanning Electron Microscopy with Energy Dispersive X-ray Spectroscopy [SEM-EDX] [FESEM-EDX, MIRA 3 TESCAN company, Czech Republic], and Fourier Transform Infrared Spectroscopy [FTIR] [IRAffinity-1S, Shimadzu, Japan]. Origin software]OriginPro 2024 v10.1.0.178, originLab[was also used to draw FTIR diagrams.

FE-SEM imaging was utilized to analyze the surface and morphological features of silk both pre- and post-coating with Ce-BT and Ce-GT. In this method, the sample was bombarded with electrons; it was studied using a 15 kV accelerating voltage.

To prepare the sample, the surface of the threads was coated with a very thin layer of gold to cause surface transfer, and then the samples were placed on the surface of the aluminum conductor. Next, an operating pressure of 7×10^{-2} bar and a current of 20 mA were applied for 2 minutes. Furthermore, Dynamic Light Scattering [DLS] [Zetasizer Nano Series, Malvern, UK] was conducted to assess complex particle size distribution, polydispersity index, and zeta potential.

To evaluate coating durability under simulated oral conditions, an acrylic tooth model was employed. The model was hydrated with artificial saliva [AS] prior to flossing. Coated floss samples were inserted into interdental spaces, and three buccopalatal movements were executed at the interproximal contact areas. Post-flossing, both the floss samples and tooth surfaces were examined *via* SEM to assess coating retention and transfer.

2.4. Tensile Strength Testing

The mechanical properties of the coated dental floss samples were evaluated using a tensile test following the ASTM D638 standard method [n = 15]. This method is widely used to determine the tensile properties of both reinforced and unreinforced plastics. The test employs a standardized dumbbell-shaped or dog-bone-shaped specimen and is conducted under controlled conditions of temperature, humidity, and strain rate. Floss specimens, each measuring 5 cm in length, were subjected to uniaxial tension using a universal testing machine [Zwick/Roell Z010, Germany] at the speed test of 10 mm/min. The tests were conducted at room temperature [23 ± 2°C] and relative humidity of 50 ± 5%.

2.5. *In Vitro* Antimicrobial Test

The antimicrobial efficacy of the coated silk threads was evaluated using the disk diffusion method against both Gram-positive [Staphylococcus aureus ATCC 25923 and Streptococcus mutans ATCC 35668] and Gram-negative [Escherichia coli ATCC 25922 and Porphyromonas gingivalis ATCC 3227] bacteria, as well as the fungus Candida albicans ATCC 10231. All microbial strains were obtained from the Pasteur Institute of Iran. Mueller-Hinton agar plates [MHA, Merck, Germany] were inoculated with standardized microbial suspensions [0.5 McFarland standard, approximately 1-2 × 10^8 CFU/mL] using sterile cotton swabs. Prior to testing, the coated silk threads were rinsed with sterile deionized water and air-dried in a laminar flow hood. Segments [2 cm] of black

tea-coated and green tea-coated silk threads were aseptically placed on the inoculated agar surfaces. The plates were then incubated at 37°C ± 1°C for 24 hours under aerobic conditions. Selective media for the growth of *P. gingivalis* and *S. mutans* was Brucella agar. The medium was supplemented with sheep blood, haemin and vitamin K to provide essential nutrients for certain anaerobes. Gentamicin disks [10 µg, Oxoid, UK] served as the positive control for bacterial strains, while fluconazole disks [25 µg, Oxoid, UK] were used for C. albicans. The diameters of the inhibition zones around the threads and control disks were measured to the nearest millimeter using digital calipers. All tests were performed in triplicate, and the results were expressed as mean ± standard deviation. Furthermore, to obtain scientific proof of the effectiveness of the Ce-BT and Ce-GT coated silk threads, a control group, *i.e.*, silk threads coated with 0.12% chlorhexidine, was added to the study so that the inhibition zone around the threads of both experimental and control groups in the agar plates containing the same microbial strains could be compared.

3. RESULTS

3.1. Morphological Characteristics

FTIR spectroscopy was employed to characterize the functional groups present in the tea and the synthesized complex. FTIR spectra of green and black tea leaves, uncoated silk thread, silk thread coated with polydopamine [PDA] and thread coated with dopamine along with Ce-BT and Ce-GT are shown in Fig. (**1**). As depicted in spectrum, all threads have the same 3 main bands due to the presence of amide groups, which correspond to amide I [1600 to 1800 cm^{-1}], amide II [1470 to 1570 cm^{-1}] and amide III [1250 to 1350 cm^{-1}]. Considering that these 3 peaks related to amide can be seen in Ce-BT and Ce-GT spectra, it can be said that the synthesized complex has no effect on the surface structure of silk thread [30-33].

In addition, in the examination of the spectrum of bare silk, due to the removal of sericin from the cocoon in the process of degumming and production of silk fabric, a wide band can be seen in the degummed silk thread around 3270 to 3280 cm^{-1}. Also, a peak at 1442 cm^{-1} was allocated to CH_2 scissoring in the backbone conformation and the N–H stretching vibration of the amide A absorption band, respectively [32, 34, 35].

Comparing bare silk and PDA coated thread, two new peaks showed up around 1618 cm^{-1} related to C=C stretching and around 1504 cm^{-1} related to N–H of indole or indoline structure upon the modification of the surface with PDA [33].

According to previous studies, the FTIR spectrum of the black and green tea leaves (Fig. **1**) exhibited several characteristic bands: A broad band at 3350 to 3450 cm^{-1},

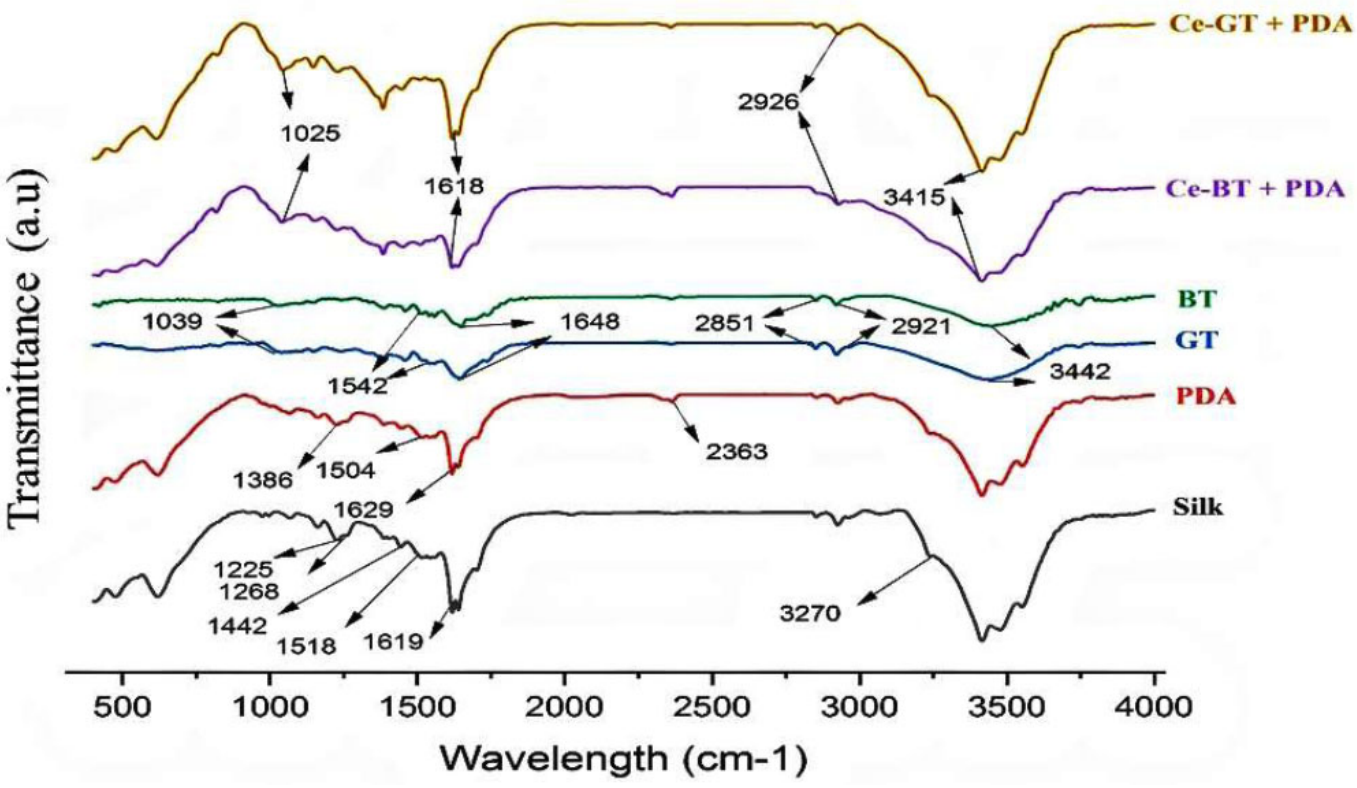

Fig. (1). FT-IR spectra of silk, PDA, GT, BT, Ce-BT and Ce-GT.

attributed to O-H and N-H stretching modes of polyphenols [36, 37]. Previously, there was confirmation that the stretching modes of N-H in [secondary and primary] amide and amine, O-H in phenols, alcohols, and carboxylic acids occupy the range of 3411 to 3370 cm^{-1} [38].

Strong absorption at 1444 to 1628 cm^{-1}, corresponding to C=O bond stretching in polyphenols and C=C bond stretching in aromatic rings [37, 39].

Bands at 2917 cm^{-1} and 2848 cm^{-1} were assigned to C-H stretch and O-H stretch of alkanes and carboxylic acids, respectively [37]. A band at 1029 cm^{-1} is indicative of C-O stretching in amino acids [37, 39].

These observations are consistent with previous studies reporting FTIR bands of tea extract polyphenols at 3388 cm^{-1} [O-H/N-H stretches], 1636 cm^{-1} [C=C], and 1039 cm^{-1} [C-O-C] [37, 39-41]. The FTIR data confirms that the main active groups in tea are polyphenols, carboxylic acids, and amino acids. The band at 1730 cm−1 was assigned to the stretching vibration of the carbonyl moiety in hemicellulose, while the band at 1700 cm−1 corresponds to the CONR stretching vibration in caffeine [42].

As it is clear from the comparison of the spectra of green and black tea, these two spectra are very similar. They differ only in terms of intensity and the presence of band 1340 cm^{-1}. This band belongs to the C-O bond present in catechins, which are found in lower quantities in black teas since they are oxidized to quinoid oligomers [43].

The FTIR spectrum of the Ce[III]-black tea complex (Fig. **1**) showed notable changes compared to the black tea leaves spectrum: The spectral bands observed in the black tea leaves spectrum reappeared in the Ce[III]-complex spectrum but with shifted intensity. Significant changes were observed in the 1700-400 cm^{-1} range, which is associated with binding and stretching vibrations of pyrimidine, carbonyl, imidazole, and methyl fragments in caffeine [44, 45]. The absorption band at 1039 cm^{-1} in the black tea spectrum almost disappeared in the Ce[III]-complex spectrum and shifted to 1025 cm^{-1}. These spectral changes, particularly in the 1700-400 cm^{-1} range, can be attributed to the coordination between Ce^{+3} cations, polyphenols, and caffeine.

Recent studies have identified theanine, catechin, caffeine, and theaflavin as the main components of black and green tea [46]. Based on our FTIR analysis and previous research [46, 47], we can confirm the formation of complexes between Ce^{3+} ions and these primary constituents of black tea extract.

Evidence supporting the successful application of the coatings was obtained by measuring the weight change after the coating process (Fig. **2A-C**). The results revealed significant increases in weight for both coating stages. The initial polydopamine coating resulted in a weight gain of approximately 1.8 mg, representing a 16.66% increase. Subsequently, the cerium tea complex coating led to an additional weight gain of around 4 mg, corresponding to a 37.03% increase from the original weight.

The surface morphology and elemental composition of the silk threads coated with the cerium-tea complex were analyzed using scanning electron microscopy [SEM]. Figs. (**3** and **4**) present the SEM micrographs of both coated and uncoated silk threads. SEM analysis revealed the presence of amorphous structures on the surface of the coated silk threads (Fig. **3A-D**), which were absent on the uncoated control threads (Fig. **3A**). The complex's amorphous structure, positioned on the silk thread and observed at a magnification of 500 nm, is illustrated in Fig. (**4A-B**).

3.2. Mechanical Properties

To assess the stability of the coating under simulated use conditions, the threads were subjected to a flossing procedure using an acrylic tooth model (Fig. **5A-D**). Post-flossing SEM analysis showed comparable fiber disruption patterns in both coated and uncoated threads. However, a notable reduction in the visible complex structures was observed on the coated threads pre-flossing images [**5Bi**, Bii], compared to after flossing (Fig. **5Ci**, **Cii**).

The tensile strength test results are shown in Fig. (**6**). The maximum acceptable stress for uncoated silk thread was found to be 21.8 MPa, whereas the stress tolerance for coated silk thread with the complex and PDA reached 28 MPa.

Examining the energy-dispersive X-ray [EDX] graphs indicates that in uncoated thread, the percentage of cerium ions is zero, but in the silk thread coated with black and green tea complex with cerium, the amount of cerium ions is significant, which indicates the success of the coating method (Fig. **3D**).

3.3. Antimicrobial Assay

The results presented in Fig. (**7A-C**) indicate that growth inhibition zones were observed only for samples 5 and 6, which correspond to the synthesized complexes. Given that green and black tea extracts alone did not exhibit significant antimicrobial activity, it can be inferred that the synthesized complexes demonstrate considerable antibacterial efficacy against *Escherichia coli, Staphylococcus aureus*, and *Candida albicans*. Also, the diameter of the inhibition zone of the commercial dental floss coated with the complex is shown in Fig. (**8A-D**).

The silk thread that has been coated with the complex demonstrates significant antibacterial properties against Streptococcus mutans and Porphyromonas gingivalis. The reported diameter of the growth inhibition zone (Fig. **9**) for S. mutans was 17.33 ± 3.21 mm for the black tea complex and 15.33 ± 1.53 mm for the green tea complex. Additionally, the values for P. gingivalis were reported as 17.33 ± 3.51 mm and 17.33 ± 1.52 mm, respectively.

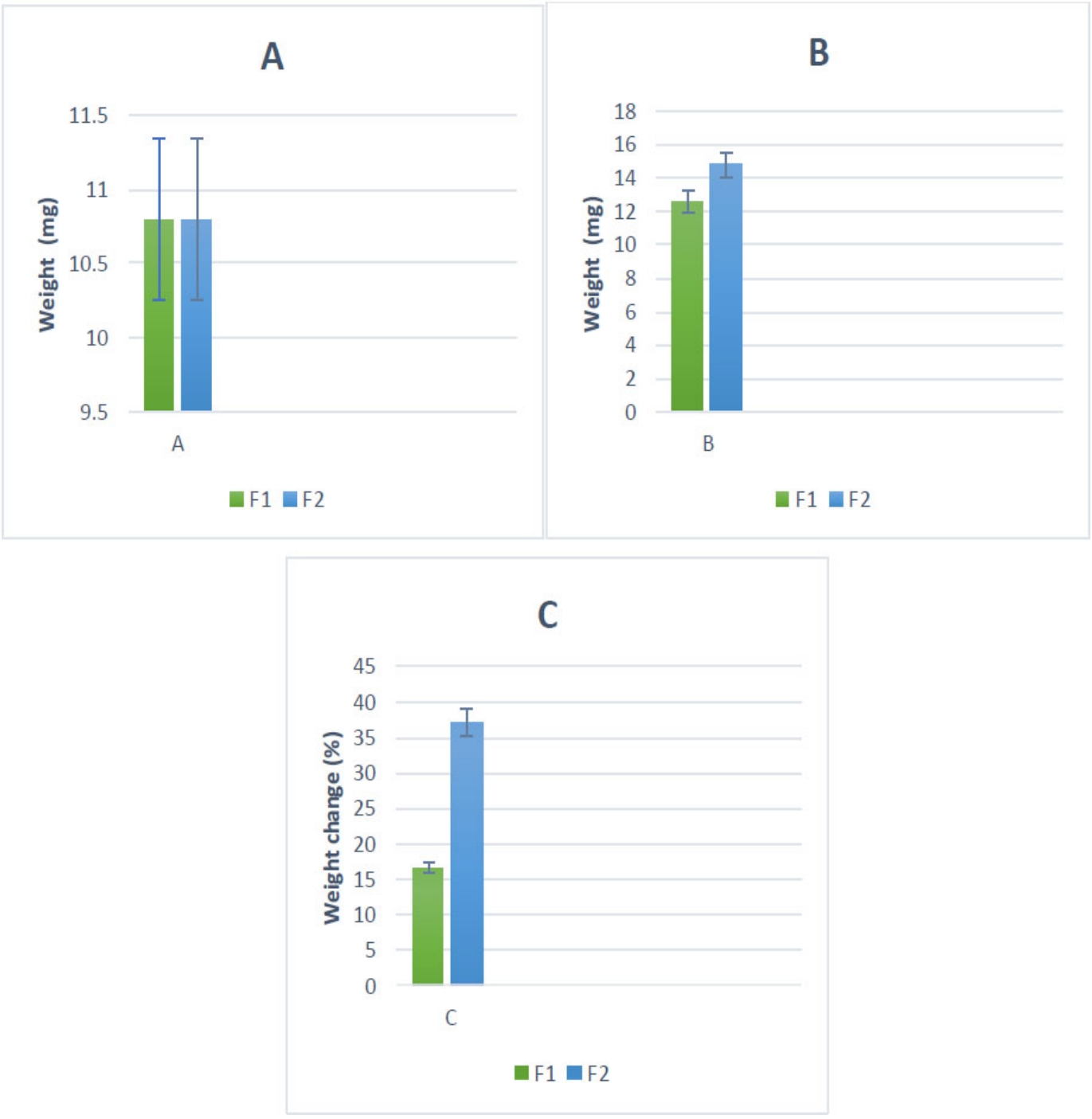

Fig. (2). Quantification of coatings on floss materials; weight before coating [**A**]; weight after coating [**B**]; and percentage weight change for PDA-coated and PDA-Cerium complex samples [**C**]. F1= silk coated with PDA, F2= silk coated with PDA+Ce-BT. The data is reported as mean ± std de.

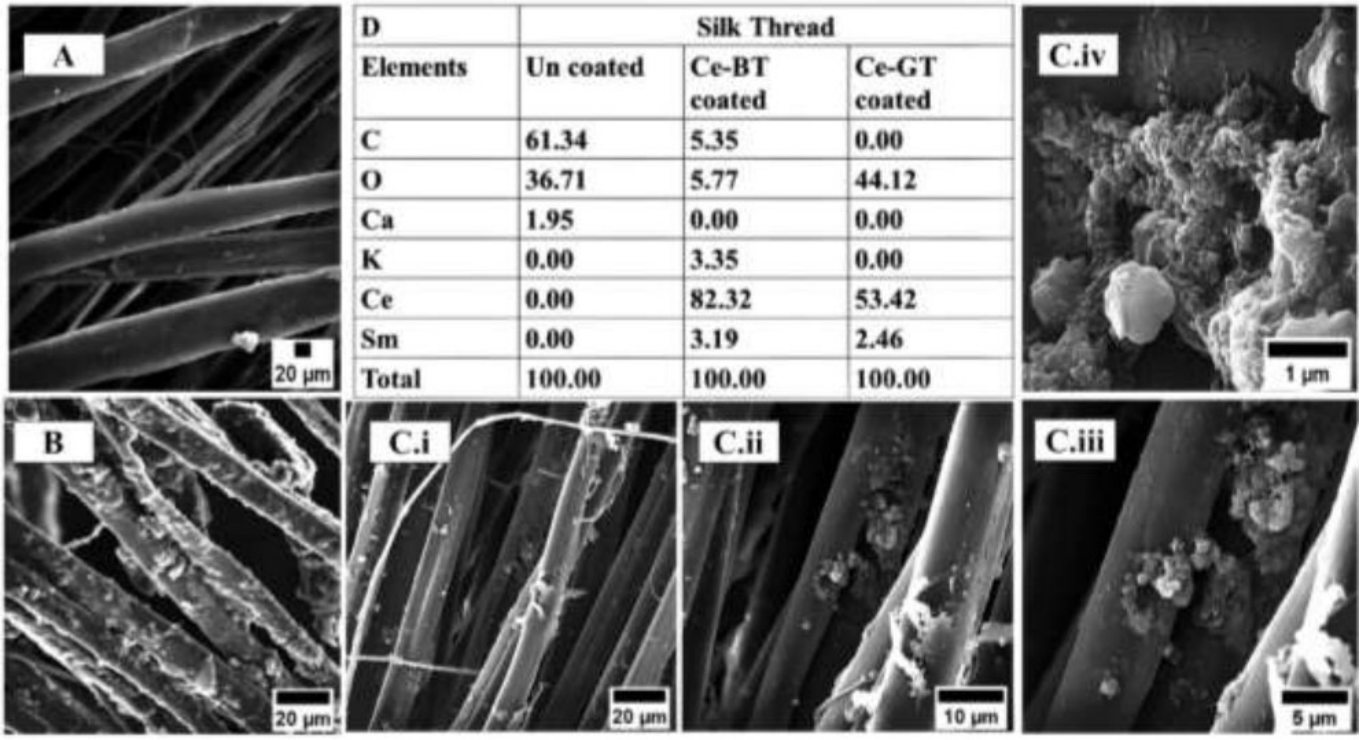

D	Silk Thread		
Elements	Un coated	Ce-BT coated	Ce-GT coated
C	61.34	5.35	0.00
O	36.71	5.77	44.12
Ca	1.95	0.00	0.00
K	0.00	3.35	0.00
Ce	0.00	82.32	53.42
Sm	0.00	3.19	2.46
Total	100.00	100.00	100.00

Fig. (3). Appearance of the floss samples before and after coating as observed by SEM; uncoated silk thread [**A**]; cerium-BT coated silk thread [**B**]; and cerium-GT coated silk thread at low [**C. i**], medium [**C. ii**] and high [**C. iii**, **C. iv**] magnification. Coated and uncoated floss compositions according to EDX [**D**].

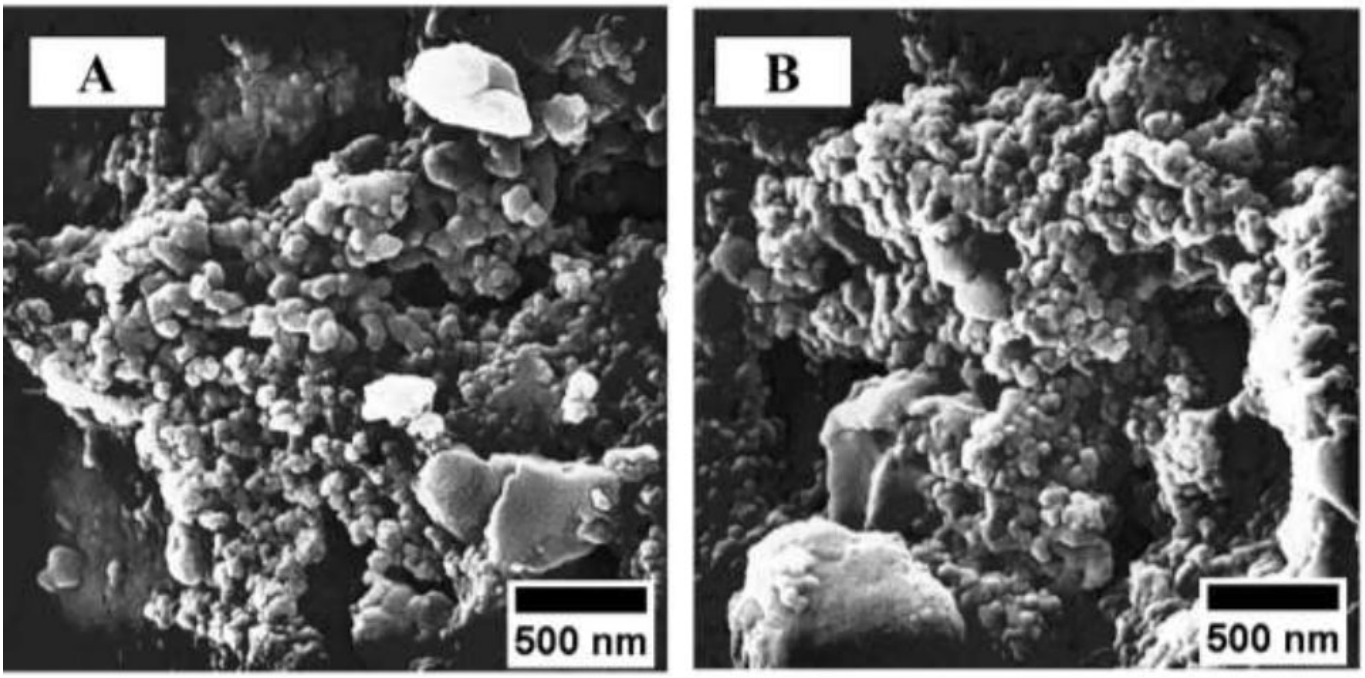

Fig. (4). Appearance of the amorphous structure of Ce-BT [**A**] and Ce-GT coated silk [**B**] at 500 nm magnification.

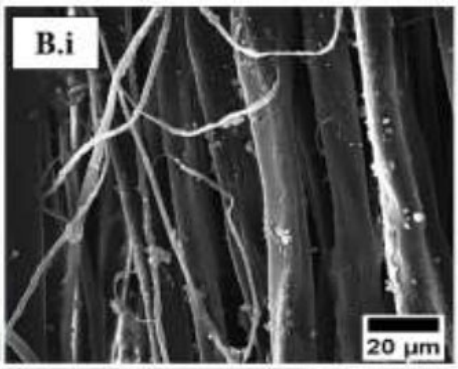

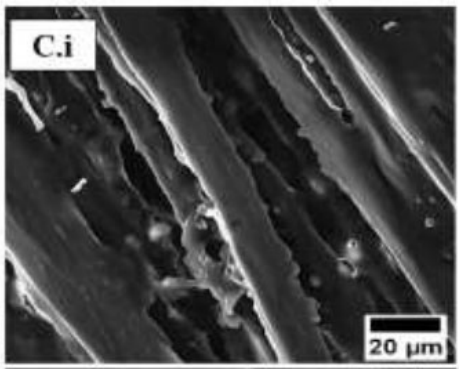

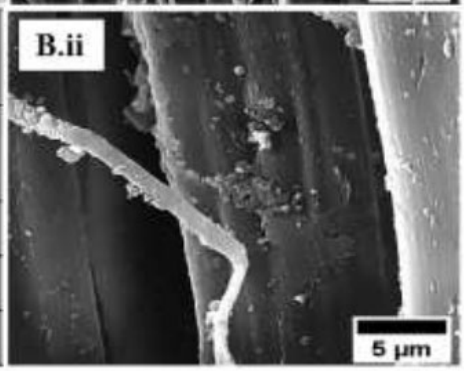

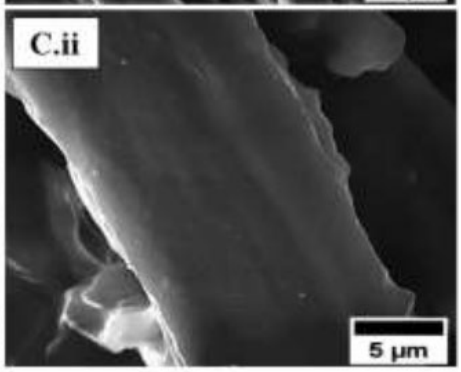

D	Silk Thread	
Elements	Before flossing	After flossing
O	52.86	72.44
Ce	47.14	27.56
Total	100.00	100.00

Fig. (5). Panel representing flossing on an artificial acrylic tooth model [**A**] and coated thread before [**B. i**, **B. ii**] and after [**C. i**, **C. ii**] flossing. Subsequent appearance of the exemplary floss, coated and uncoated floss compositions according to EDX and before and after flossing composition [D] that provides qualitative evidence of transfer of the cerium-complex coating from the floss to the tooth surface.

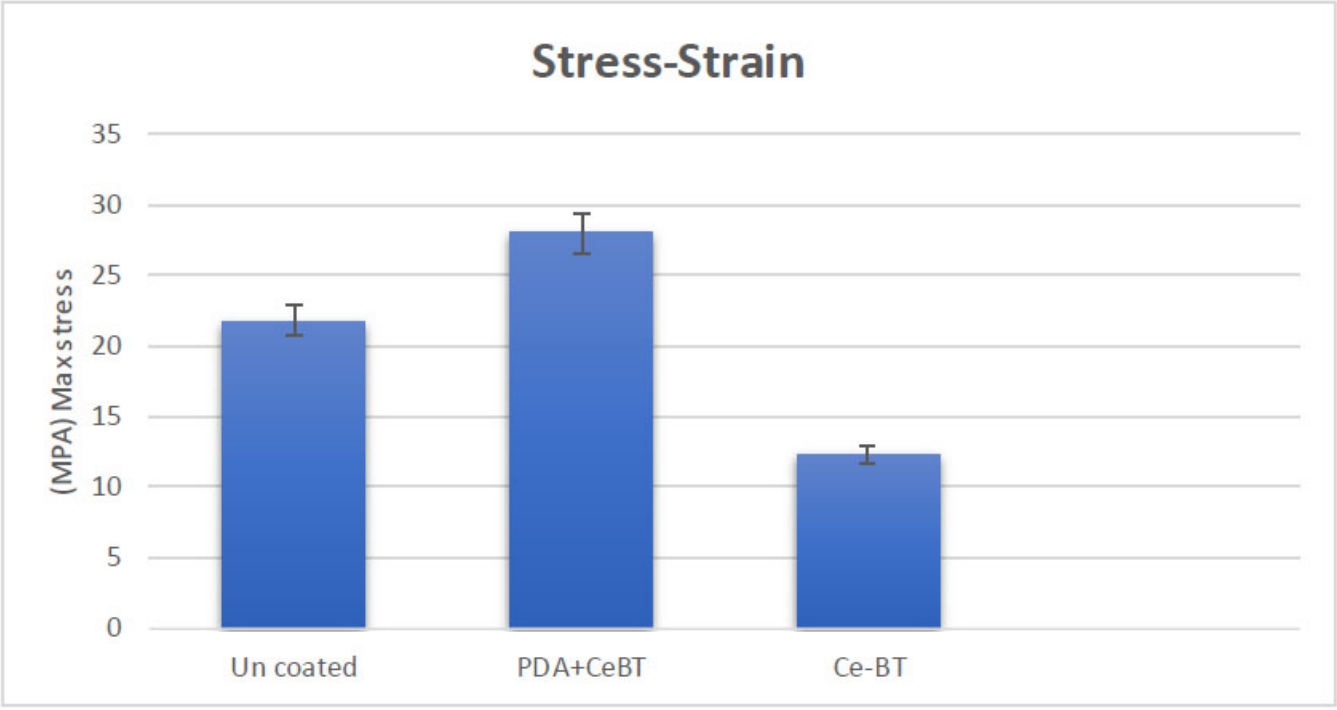

Fig. (6). The impact of the coating procedure on tensile strength.

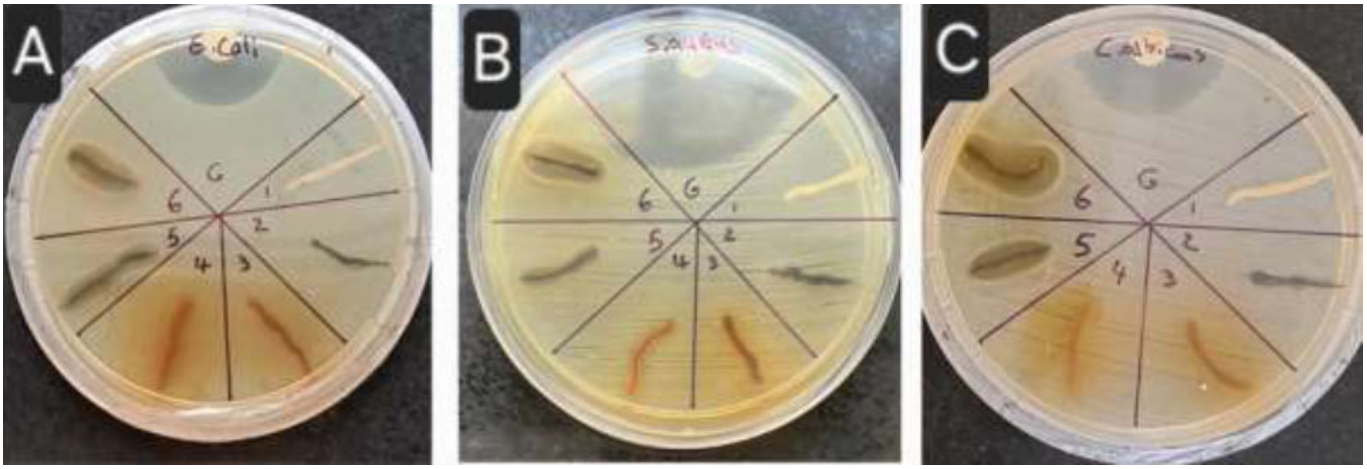

Fig. (7). 1: uncoated thread, 2: PDA coated thread, 3: coated with black tea extract, 4: coated with green tea extract, 5: Ce-BT+PDA coated thread, 6: Ce-GT+PDA coated thread.
A: *E. coli*, **B**: *S. aureus*, **C**: *C. albicans*.

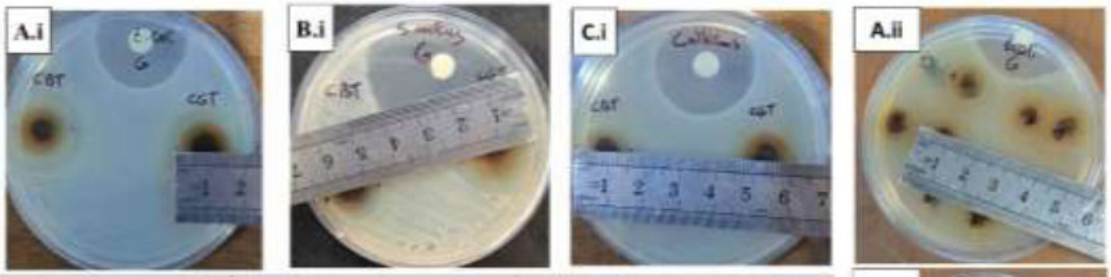

D	*E. coli* (mm)		*S. aureus* (mm)		*C. albicans* (mm)	
	Ce-BT	Ce-GT	Ce-BT	Ce-GT	Ce-BT	Ce-GT
Silk thread	14.66 ± 1.52	15.66 ± 1.52	16.66 ± 2.88	16.33 ± 1.52	13.66 ± 1.52	14.33 ± 1.52
Oral B	5.67 ± 0.58	6.33 ± 0.58	6.66 ± 1.15	9.33 ± 0.57	0.00	6 ± 1
Oral B Satin	5.67 ± 0.58	9.67 ± 1.15	10.33 ± 1.15	11.33 ± 1.52	0.00	0.00
MISSWAKE	9.33 ± 0.58	11 ± 1	12.66 ± 0.58	13 ± 1	10.67 ± 0.58	11 ± 1
Vi-one	12 ± 1.73	12 ± 1	14.33 ± 0.58	16 ± 1	10.67 ± 1.15	11.33 ± 1.15

Fig. (8). Measurement and comparison of the diameter of the inhibition zones. Silk thread [**A.i**, **B.i**, **C.i**] and commercial dental floss [**A.ii**, **B.ii**, **C.ii**].

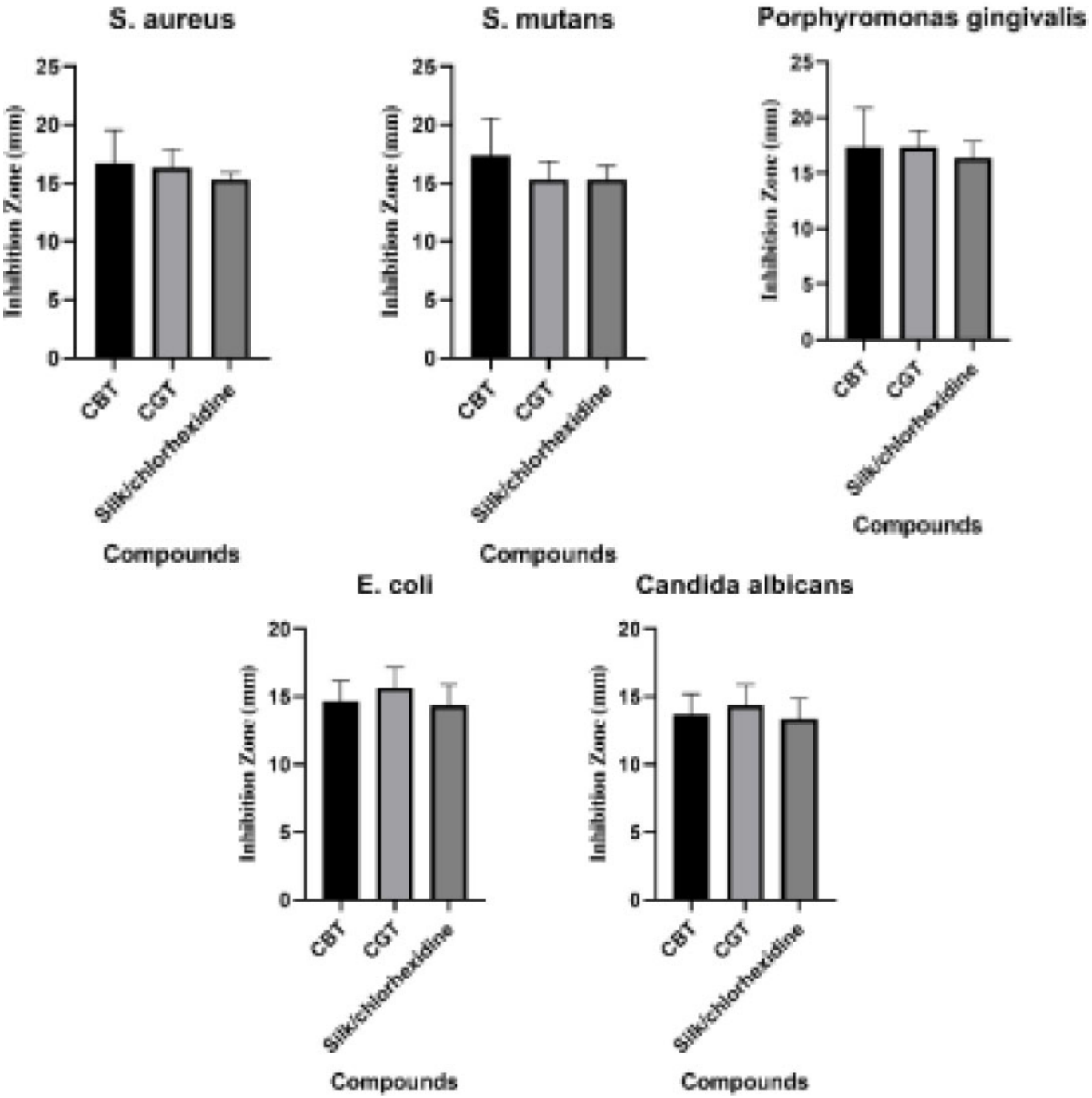

Fig. (9). Inhibition zones for *S. aureus*, *S. mutans*, *P. gingivalis*, *E. coli* and *C. albicans*.

The results presented in Fig. (**9**) and Table **1** indicate that the diameter of the growth inhibition zone in the silk thread coated with the complex is more than the sample coated with chlorhexidine, so the antibacterial property of the synthesized complex is more than 0.12% chlorhexidine. However, the results of one-way ANOVA tests conducted in GraphPad Prism version 10.4.1 [627] comparing the inhibition zone of the microbial strains around Ce-BT, Ce-GT, and chlorhexidine silk threads indicate that the experimental group threads and control group thread are not significantly different in their antimicrobial property (Table **2**). Despite the insignificance of their difference, Ce-BT and Ce-GT coated thread are superior to chlorhexidine coated threads in that they have a relatively bigger inhibition zone, they are natural and green synthesized, and chlorhexidine is known to leave stains on the teeth.

Table 1. Inhibition zones for the microbial strains around Ce-BT, Ce-GT, and chlorhexidine silk threads.

-	*S. aureus* [mm]	*S. mutans* [mm]	*P. gingivalis* [mm]	*E. coli* [mm]	*C. albicans* [mm]
CBT	16.66 ± 2.88	17.33 ± 3.21	17.33 ± 3.51	14.66 ± 1.52	13.66 ± 1.52
CGT	16.33 ± 1.52	15.33 ± 1.53	17.33 ± 1.52	15.66 ± 1.52	14.33 ± 1.52
Silk/chlorhexidine	15.33 ± 0.57	15.33 ± 1.15	16.33 ± 1.52	14.33 ± 1.52	13.33 ± 1.52

Table 2. *p*-value of experimental and control group threads comparison using one-way ANOVA.

p-value	*S. aureus*	*S. mutans*	*P. gingivalis*	*E. coli*	*C. albicans*
Silk/chlorhexidine *vs*. CBT	0.6261	0.4642	0.8317	0.9496	0.9496
Silk/chlorhexidine *vs*. CGT	0.7578	>0.9999	0.8317	0.4993	0.6575

3.4. Particle Size Distribution

Particle size distribution analysis was conducted on both the cerium nanoparticles [CeNPs] and the synthesized Ce-BT using DLS. The results of these measurements are presented in Fig. (**10**), with panel A showing the distribution of the Ce-BT complex and panel B displaying the distribution of the cerium nanoparticles.

The DLS measurements revealed that the cerium nanoparticles (Fig. **10A**) had a mean hydrodynamic diameter of 306 nm. This size falls within the upper range of the nanoparticle classification, suggesting that some agglomeration may have occurred or that the particles have a non-spherical shape, leading to a larger hydrodynamic radius.

In contrast, the synthesized Ce-BT complex (Fig. **10B**) exhibited a larger mean hydrodynamic diameter of 578 nm. This nearly twofold increase in size compared to the bare CeNPs indicates successful complexation between the cerium nanoparticles and tea molecules. The larger size of the complex can be attributed to the attachment of BT molecules to the surface of the CeNPs, as well as possible cross-linking between particles mediated by the BT molecules.

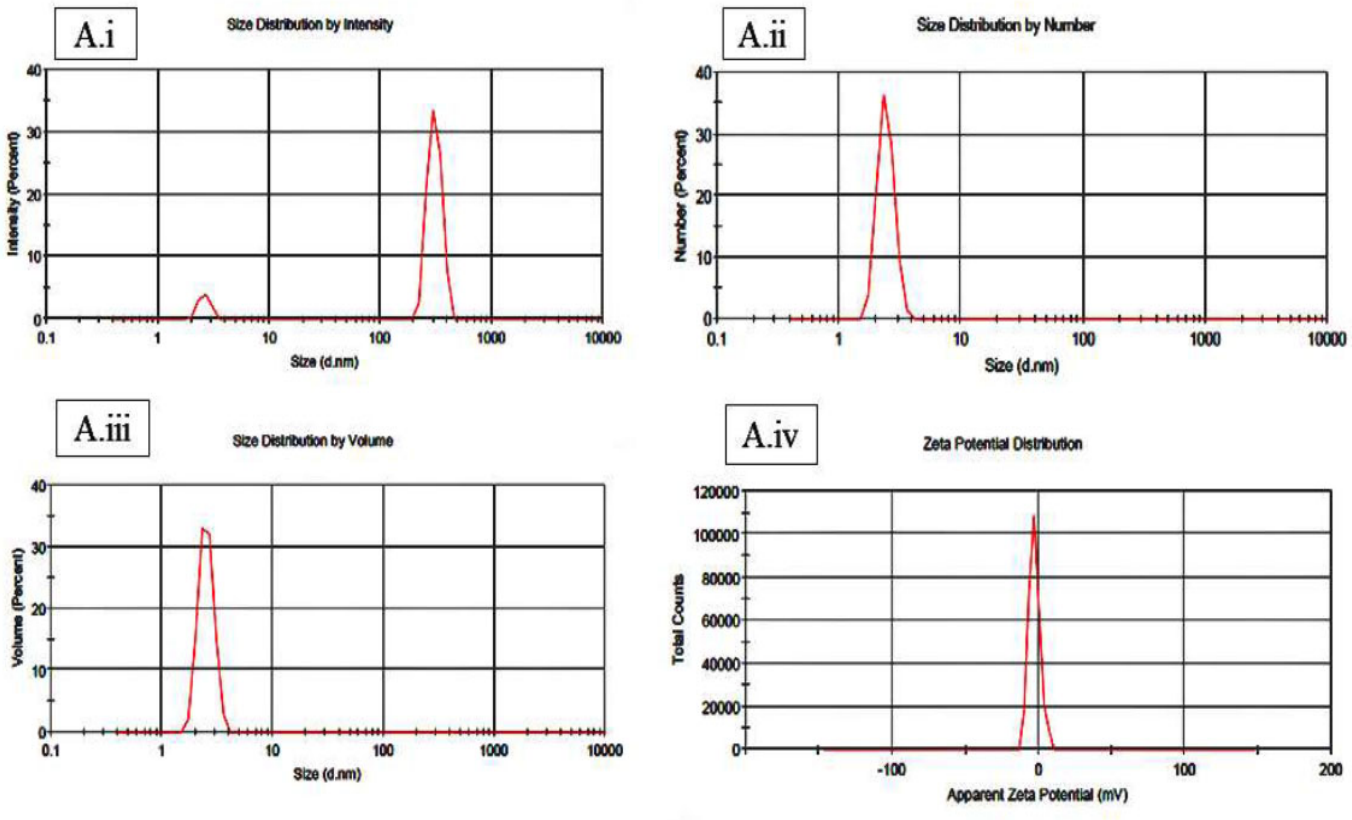

Fig. 10 contd.....

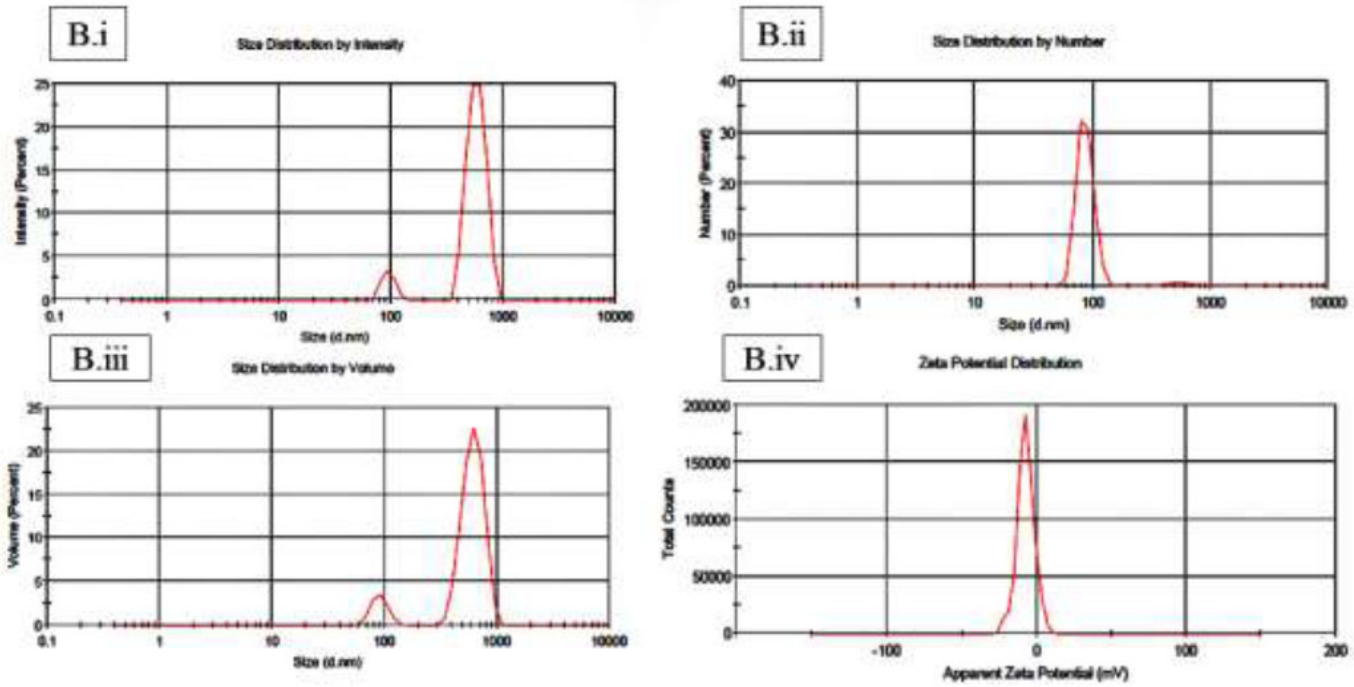

Fig. (10). Dynamic Light Scattering [DLS] analysis of **A** [i-iv] Ce-BT complex and **B** [i-iv] cerium nanoparticles [CeNPs].

4. DISCUSSION

Research indicates that following the treatment of active periodontitis, the persistence of periodontal pockets in the subgingival region poses a significant risk for the re-emergence of inflammation and the advancement of the disease. Consequently, effective management of periodontitis necessitates ongoing, lifelong care [4].

This study presents a novel approach to enhancing dental floss functionality through a dual-layer coating of polydopamine and cerium tea complex.

Our method utilized a green synthesis approach, employing tea extract solutions to produce a stable cerium complex cost-effectively. Spectroscopic analyses confirmed the successful interaction between cerium ions and tea polyphenols. Microscopy and elemental analysis verified the effective coating of the floss with the synthesized complex.

Observations of the floss before and after use indicated that the coating readily transfers in the oral environment, potentially enabling it to exert its antibacterial and anti-inflammatory effects. Antibacterial tests corroborated these properties, while mechanical tests confirmed that the coated floss maintained appropriate strength and durability for dental applications. Cytotoxicity assays verified the biocompatibility of the cerium-based coating with mammalian cells.

The spectroscopic evidence (Fig. **1**) supports the successful synthesis of Ce[III]-black tea complexes, providing insight into the molecular interactions involved in their formation. According to the results of weight changes (Fig. **2**), it can be seen that these weight gains are notably higher than those reported in previous studies involving antibiotic coatings on dental floss for periodontal applications [48]. The substantial difference in coating mass can be attributed to the unique properties of polydopamine and cerium tea complex, as well as the direct application method used in this study.

The choice of polydopamine as the initial coating was deliberate, given its well-documented ability to adhere to various surfaces and its potential to enhance the bonding between the cerium tea complex and the nylon floss material. The subsequent cerium tea complex coating was selected for its anticipated antibacterial and protective properties, which could prove beneficial in oral care applications.

According to the SEM results in Figs. (**3** and **4**), this observation suggests successful adsorption of the synthesized cerium-tea complex onto the thread surface. Elemental analysis *via* EDS corroborated these observations. Comparative EDS spectra of coated threads before and after flossing demonstrated a significant decrease in cerium content post-flossing (Fig. **5D**). This quantitative data further supports the hypothesis of coating transfer during the flossing procedure. These findings collectively indicate successful complex synthesis, effective thread coating, and potential release of the active compounds during simulated dental hygiene practices. This decrease in surface coating suggests a potential transfer of the complex into the interdental and interproximal spaces of the tooth model during the flossing process (Fig. **5B**, **C**). Polydopamine and cerium tea complex coatings were successfully deposited into the spaces between teeth and along the gum line during the flossing process. This transfer of coating material mirrors findings from other studies, where researchers were able to detect the presence of fluorescent-tagged substances

on both dental and gingival surfaces after using floss treated with experimental coatings [48].

This transfer effect could be particularly beneficial. The polydopamine base layer, known for its adhesive properties, may facilitate the adherence of the cerium tea complex to oral tissues. This could potentially lead to prolonged contact between the active compounds and the target areas, possibly enhancing the effectiveness of the treatment. In addition, as in Fig. (**6**). It is known that the PDA layer increases the mechanical resistance against stretching.

In several previous studies, it has been proven that the coating of experimental dental floss with novel coatings materials did not change the mechanical properties of the dental floss [9, 49], but during the results obtained from the strain stress test, it was found that the floss coated with the synthesized complex compared to Uncoated thread has higher strength and resistance. Also, by comparing the max stress in the thread coated with the complex and the thread coated with the complex along with PDA, it was found that the presence of the PDA layer has significant effects in increasing the strength of the thread.

In the evaluation of antibacterial outcomes, the data suggest that the Ce-GT [Cerium-Green Tea] complex exhibits strong antimicrobial properties, while the Ce-BT [Cerium-Black Tea] complex shows comparatively weaker effects. This indicates that the Ce-GT complex possesses superior antibacterial properties compared to Ce-BT. These findings align with previous research, which suggests an inverse relationship between the degree of tea fermentation and antibacterial activity. Consequently, green tea, being less fermented, demonstrates stronger antibacterial properties than black tea [50, 51]. How the diameter of the inhibition zones is measured is shown in Fig. (**8**).

However, it could be interesting in the future to test green tea in combination with other recently introduced adjunctive treatments such as Ozone [52], photobiomodulation [53], and paraprobiotics [54] in order to understand their mutual effect on periodontal tissues.

The potential for integrating this technology into daily oral hygiene routines is promising. Such preventive oral health products are highly desirable compared to more invasive curative treatments or dental rehabilitation procedures. The over-the-counter nature of this product could promote widespread adoption without requiring professional dental intervention.

However, to fully realize this potential, future research should address certain limitations of the current study. For instance, optimizing the coating process using specialized fiber holders could enhance coating uniformity and quality. Subsequent studies should also focus on testing the efficacy against specific oral pathogens associated with dental caries and periodontal diseases. More comprehensive evaluations, including antifungal effects and time-kill assays, would provide valuable insights into the product's effectiveness. Additionally, performing *in vivo* tests on rat teeth or porcine gum would enable further investigation into the antioxidant and antibacterial properties of the synthesized dental floss.

Advanced studies quantifying the deposition of the cerium tea complex on proximal tooth surfaces and monitoring its effects on remineralization and early caries arrest in both *in vitro* and animal models would offer more predictive data on potential clinical outcomes. The possibility of incorporating additional biologically active and antibacterial ions into the coating remains an intriguing avenue for future exploration.

CONCLUSION

Our research demonstrates, for the first time, the potential of this coating combination to improve the antibacterial properties of dental floss while maintaining its mechanical integrity. This innovation suggests that dental floss can effectively serve as a delivery system for antibacterial compounds directly into interdental spaces.

From a therapeutic standpoint, this specialized floss could offer an effective approach to treating subgingival infections by delivering antibacterial and anti-inflammatory agents directly to affected areas, addressing a significant challenge in periodontitis treatment. We anticipate that further research, potentially incorporating additional natural agents to enhance its properties, could expand the applications of this cerium tea complex coating to other medical fields, such as antibacterial sutures, wound dressings, and burn treatments.

AUTHORS' CONTRIBUTIONS

The authors confirm their contribution to the paper: S.H.: Study conception and design; S.S.: Data collection; P.A.: Analysis, and interpretation of results; Z.E.M.: Draft manuscript. All authors reviewed the results and approved the final version of the manuscript.

ETHICS APPROVAL AND CONSENT TO PARTICIPATE

Not applicable.

HUMAN AND ANIMAL RIGHTS

Not applicable.

CONSENT FOR PUBLICATION

Not applicable.

AVAILABILITY OF DATA AND MATERIALS

All the data and supporting information are provided within the article.

FUNDING

None.

CONFLICT OF INTEREST

The authors declare no conflict of interest, financial or otherwise.

ACKNOWLEDGEMENTS

Declared none.

REFERENCES

[1] Nibali L, D'Aiuto F, Griffiths G, Patel K, Suvan J, Tonetti MS. Severe periodontitis is associated with systemic inflammation and a dysmetabolic status: A case–control study. J Clin Periodontol 2007; 34(11): 931-7.

http://dx.doi.org/10.1111/j.1600-051X.2007.01133.x PMID: 17877746
[2] Li X, Kolltveit KM, Tronstad L, Olsen I. Systemic diseases caused by oral infection. Clin Microbiol Rev 2000; 13(4): 547-58. http://dx.doi.org/10.1128/CMR.13.4.547 PMID: 11023956
[3] Lamont RJ, Koo H, Hajishengallis G. The oral microbiota: Dynamic communities and host interactions. Nat Rev Microbiol 2018; 16(12): 745-59. http://dx.doi.org/10.1038/s41579-018-0089-x PMID: 30301974
[4] Nakajima M, Nakajima N, Guo J, Mitragotri S. Engineering of bioactive nanocomplexes on dental floss for targeted gingival therapy. Bioeng Transl Med 2023; 8(2): e10452. http://dx.doi.org/10.1002/btm2.10452 PMID: 36925712
[5] Sälzer S, Slot DE, Van der Weijden FA, Dörfer CE. Efficacy of inter-dental mechanical plaque control in managing gingivitis – A meta-review. J Clin Periodontol 2015; 42(S16): S92-S105. http://dx.doi.org/10.1111/jcpe.12363 PMID: 25581718
[6] Cepeda MS, Weinstein R, Blacketer C, Lynch MC. Association of flossing/inter-dental cleaning and periodontitis in adults. J Clin Periodontol 2017; 44(9): 866-71. http://dx.doi.org/10.1111/jcpe.12765 PMID: 28644512
[7] Berchier CE, Slot DE, Haps S, Van der Weijden GA. The efficacy of dental floss in addition to a toothbrush on plaque and parameters of gingival inflammation: A systematic review. Int J Dent Hyg 2008; 6(4): 265-79. http://dx.doi.org/10.1111/j.1601-5037.2008.00336.x PMID: 19138178
[8] Matzeu G, Naveh GRS, Agarwal S, *et al*. Functionalized mouth-conformable interfaces for pH evaluation of the oral cavity. Adv Sci (Weinh) 2021; 8(12): 2003416. http://dx.doi.org/10.1002/advs.202003416 PMID: 34165900
[9] Boese S, Gill HS. Drug-coated floss to treat gum diseases: *in vitro* and *in vivo* characterization. ACS Appl Mater Interfaces 2022; 14(25): 28663-70. http://dx.doi.org/10.1021/acsami.2c07976 PMID: 35708223
[10] Kaewiad K, Nakpheng T, Srichana T. Dental floss impregnated with povidone-iodine coated with Eudragit L-100 as an antimicrobial delivery system against periodontal-associated pathogens. J Med Microbiol 2020; 69(2): 298-308. http://dx.doi.org/10.1099/jmm.0.001126 PMID: 31976854
[11] Muniz FWMG, da Silva Lima H, Rösing CK, Martins RS, Moreira MMSM, Carvalho RS. Efficacy of an unwaxed dental floss impregnated with 2% chlorhexidine on control of supragingival biofilm: A randomized, clinical trial. J Investig Clin Dent 2018; 9(1): e12280. http://dx.doi.org/10.1111/jicd.12280 PMID: 28691316
[12] Muniz FWMG, Sena KS, de Oliveira CC, Veríssimo DM, Carvalho RS, Martins RS. Efficacy of dental floss impregnated with chlorhexidine on reduction of supragingival biofilm: A randomized controlled trial. Int J Dent Hyg 2015; 13(2): 117-24. http://dx.doi.org/10.1111/idh.12112 PMID: 25376536
[13] Boronow KE, Brody JG, Schaider LA, Peaslee GF, Havas L, Cohn BA. Serum concentrations of PFASs and exposure-related behaviors in African American and non-Hispanic white women. J Expo Sci Environ Epidemiol 2019; 29(2): 206-17. http://dx.doi.org/10.1038/s41370-018-0109-y PMID: 30622332
[14] Kelekis-Cholakis A, Perry JB, Pfeffer L, Millete A. Successful treatment of generalized refractory chronic periodontitis through discontinuation of waxed or coated dental floss use. J Am Dent Assoc 2016; 147(12): 974-8. http://dx.doi.org/10.1016/j.adaj.2016.06.009 PMID: 27423761
[15] Grossman E, Hou L, Bollmer BW, *et al*. Triclosan/pyrophosphate dentifrice: Dental plaque and gingivitis effects in a 6-month randomized controlled clinical study. J Clin Dent 2002; 13(4): 149-57. PMID: 12116725
[16] Yang H, Wang W, Romano KA, *et al*. A common antimicrobial additive increases colonic inflammation and colitis-associated colon tumorigenesis in mice. Sci Transl Med 2018; 10(443): eaan4116. http://dx.doi.org/10.1126/scitranslmed.aan4116 PMID: 29848663
[17] Traitanon N, Dechkunakorn S, Tantivitayakul P. Antibacterial effect of gold nanoparticles coated dental floss against cariogenic bacteria. KEM 2021; 904: 293-300. http://dx.doi.org/10.4028/www.scientific.net/KEM.904.293
[18] Boese S, Gill HS. Coated floss for drug delivery into the gum pocket. Int J Pharm 2021; 606: 120855. http://dx.doi.org/10.1016/j.ijpharm.2021.120855 PMID: 34224840
[19] Haidar ZS. Dental floss for preventing or treating dental caries and periodontal disease. 2022. Google Patents
[20] Barker E, Shepherd J, Asencio IO. The use of cerium compounds as antimicrobials for biomedical applications. Molecules 2022; 27(9): 2678. http://dx.doi.org/10.3390/molecules27092678 PMID: 35566026
[21] Varghese EJ, Sihivahanan D, Venkatesh KV. Development of novel antimicrobial dental composite resin with nano cerium oxide fillers. Int J Biomater 2022; 2022(1): 1-7. http://dx.doi.org/10.1155/2022/3912290 PMID: 35464636
[22] Santhosh PB, Genova J, Chamati H. Green synthesis of gold nanoparticles: An eco-friendly approach. Chemistry 2022; 4(2): 345-69. http://dx.doi.org/10.3390/chemistry4020026
[23] Nadeem M, Abbasi BH, Younas M, Ahmad W, Khan T. A review of the green syntheses and anti-microbial applications of gold nanoparticles. Green Chem Lett Rev 2017; 10(4): 216-27. http://dx.doi.org/10.1080/17518253.2017.1349192
[24] Usman AI, Abdul Aziz A, Abu Noqta O. Application of green synthesis of gold nanoparticles: A review. J Teknol 2018; 81(1) http://dx.doi.org/10.11113/jt.v81.11409
[25] Ciraldo FE, Schnepf K, Goldmann WH, Boccaccini AR. Development and characterization of bioactive glass containing composite coatings with ion releasing function for antibiotic-free antibacterial surgical sutures. Materials (Basel) 2019; 12(3): 423. http://dx.doi.org/10.3390/ma12030423 PMID: 30704083
[26] Schuhladen K, Raghu SNV, Liverani L, Neščáková Z, Boccaccini AR. Production of a novel poly(ε-caprolactone)-methylcellulose electrospun wound dressing by incorporating bioactive glass and Manuka honey. J Biomed Mater Res B Appl Biomater 2021; 109(2): 180-92. http://dx.doi.org/10.1002/jbm.b.34690 PMID: 32691500
[27] Iravani S. Green synthesis of metal nanoparticles using plants. Green Chem 2011; 13(10): 2638-50. http://dx.doi.org/10.1039/c1gc15386b
[28] Brza MA, Aziz SB, Anuar H, *et al*. Tea from the drinking to the synthesis of metal complexes and fabrication of PVA based polymer composites with controlled optical band gap. Sci Rep 2020; 10(1): 18108. http://dx.doi.org/10.1038/s41598-020-75138-x PMID: 33093604
[29] Zhang W, Wang S, Ge S, Chen J, Ji P. The relationship between substrate morphology and biological performances of nano-silver-loaded dopamine coatings on titanium surfaces. R Soc Open Sci 2018; 5(4): 172310. http://dx.doi.org/10.1098/rsos.172310 PMID: 29765680
[30] Kesornsit S, Jitjankarn P, Sajomsang W, Gonil P, Bremner JB, Chairat M. Polydopamine-coated silk yarn for improving the light fastness of natural dyes. Color Technol 2019; 135(2): 143-51. http://dx.doi.org/10.1111/cote.12390
[31] Aksakal B, Koç K, Yargı Ö, Tsobkallo K. Effect of UV-light on the uniaxial tensile properties and structure of uncoated and TiO2 coated Bombyx mori silk fibers. Spectrochim Acta A Mol Biomol Spectrosc 2016; 152: 658-65. http://dx.doi.org/10.1016/j.saa.2015.01.131 PMID: 25746557
[32] Peng C, Shu Z, Zhang C, Chen X, Wang M, Fan L. Surface modification of silk fibroin composite bone scaffold with polydopamine coating to enhance mineralization ability and biological activity for bone tissue engineering. J Appl Polym Sci 2022; 139(38): e52900. http://dx.doi.org/10.1002/app.52900
[33] Lu Z, Xiao J, Wang Y, Meng M. *In situ* synthesis of silver nanoparticles uniformly distributed on polydopamine-coated silk

fibers for antibacterial application. J Colloid Interface Sci 2015; 452: 8-14.
http://dx.doi.org/10.1016/j.jcis.2015.04.015 PMID: 25909867

[34] Hamai R, Sakai S, Shiwaku Y, *et al*. Octacalcium phosphate crystals including a higher density dislocation improve its materials osteogenecity. Appl Mater Today 2022; 26: 101279. http://dx.doi.org/10.1016/j.apmt.2021.101279

[35] Ko E, Lee JS, Kim H, *et al*. Electrospun silk fibroin nanofibrous scaffolds with two-stage hydroxyapatite functionalization for enhancing the osteogenic differentiation of human adipose-derived mesenchymal stem cells. ACS Appl Mater Interfaces 2018; 10(9): 7614-25.
http://dx.doi.org/10.1021/acsami.7b03328 PMID: 28475306

[36] Loo YY, Chieng BW, Nishibuchi M, Radu S. Synthesis of silver nanoparticles by using tea leaf extract from *Camellia sinensis*. Int J Nanomedicine 2012; 7: 4263-7.
PMID: 22904632

[37] Senthilkumar S, Sivakumar T. Green tea (*Camellia sinensis*) mediated synthesis of zinc oxide (ZnO) nanoparticles and studies on their antimicrobial activities. Int J Pharm Pharm Sci 2014; 6(6): 461-5.

[38] Muheddin DQ, Aziz SB, Mohammed PA. Variation in the optical properties of PEO-based composites *via* a green metal complex: Macroscopic measurements to explain microscopic quantum transport from the valence band to the conduction band. Polymers (Basel) 2023; 15(3): 771.
http://dx.doi.org/10.3390/polym15030771 PMID: 36772071

[39] Dubey S, Sillanpaa M, Varma R. Reduction of hexavalent chromium using *Sorbaria sorbifolia* aqueous leaf extract. Appl Sci (Basel) 2017; 7(7): 715.
http://dx.doi.org/10.3390/app7070715

[40] Huang L, Weng X, Chen Z, Megharaj M, Naidu R. Synthesis of iron-based nanoparticles using oolong tea extract for the degradation of malachite green. Spectrochim Acta A Mol Biomol Spectrosc 2014; 117: 801-4.
http://dx.doi.org/10.1016/j.saa.2013.09.054 PMID: 24094918

[41] Weng X, Huang L, Chen Z, Megharaj M, Naidu R. Synthesis of iron-based nanoparticles by green tea extract and their degradation of malachite. Ind Crops Prod 2013; 51: 342-7.
http://dx.doi.org/10.1016/j.indcrop.2013.09.024

[42] Giorgini E, Notarstefano V, Foligni R, Carloni P, Damiani E. First ATR-FTIR characterization of black, green and white teas (*Camellia sinensis*) from european tea gardens: A PCA analysis to differentiate leaves from the in-cup infusion. Foods 2023; 13(1): 109.
http://dx.doi.org/10.3390/foods13010109 PMID: 38201143

[43] Balentine DA, Wiseman SA, Bouwens LCM. The chemistry of tea flavonoids. Crit Rev Food Sci Nutr 1997; 37(8): 693-704.
http://dx.doi.org/10.1080/10408399709527797 PMID: 9447270

[44] Ucun F, Sağlam A, Güçlü V. Molecular structures and vibrational frequencies of xanthine and its methyl derivatives (caffeine and theobromine) by ab initio Hartree–Fock and density functional theory calculations. Spectrochim Acta A Mol Biomol Spectrosc 2007; 67(2): 342-9.
http://dx.doi.org/10.1016/j.saa.2006.07.029 PMID: 16942910

[45] Mohamed EA, Hicham EH. Synthesis and characterization of caffeine complexes [M (Caf) 4x2] M= Ni (Ii), Cu (Ii), Zn (Ii), Cd (Ii) X= Scn-, Cn-; Caf: Caffeine. Res J Chem Sci 2014; 2231: 606.

[46] Jain H, Chella N. Methods to improve the solubility of therapeutical natural products: A review. Environ Chem Lett 2021; 19(1): 111-21.
http://dx.doi.org/10.1007/s10311-020-01082-x

[47] Wu D, Bird MR. The interaction of protein and polyphenol species in ready to drink black tea liquor production. J Food Process Eng 2010; 33(3): 481-505.
http://dx.doi.org/10.1111/j.1745-4530.2008.00286.x

[48] Altintig E, Onaran M, Sarı A, Altundag H, Tuzen M. Preparation, characterization and evaluation of bio-based magnetic activated carbon for effective adsorption of malachite green from aqueous solution. Mater Chem Phys 2018; 220: 313-21.
http://dx.doi.org/10.1016/j.matchemphys.2018.05.077

[49] Babayevska N, Woźniak-Budych M, Litowczenko J, *et al*. Novel nanosystems to enhance biological activity of hydroxyapatite against dental caries. Mater Sci Eng C 2021; 124: 112062.
http://dx.doi.org/10.1016/j.msec.2021.112062 PMID: 33947556

[50] Tiwari TP, Bharti SK, Kaur HD, Dikshit RP, Hoondal GS. Synergistic antimicrobial activity of tea & antibiotics. Indian J Med Res 2005; 122(1): 80-4.
PMID: 16106094

[51] Almajano MP, Carbó R, Jiménez JAL, Gordon MH. Antioxidant and antimicrobial activities of tea infusions. Food Chem 2008; 108(1): 55-63.
http://dx.doi.org/10.1016/j.foodchem.2007.10.040

[52] Scribante A, Gallo S, Pascadopoli M, Frani M, Butera A. Ozonized gels vs chlorhexidine in non-surgical periodontal treatment: A randomized clinical trial. Oral Dis 2024; 30(6): 3993-4000.
http://dx.doi.org/10.1111/odi.14829 PMID: 38047757

[53] Elbay M, Elbay ÜŞ, Kaya E, Kalkan ÖP. Effects of photobiomodulation with different application parameters on injection pain in children: A randomized clinical trial. J Clin Pediatr Dent 2023; 47(4): 54-62.
PMID: 37408347

[54] Butera A, Pascadopoli M, Nardi MG, *et al*. Clinical use of paraprobiotics for pregnant women with periodontitis: Randomized clinical trial. Dent J 2024; 12(4): 116.
http://dx.doi.org/10.3390/dj12040116 PMID: 38668028